BIODIVERSITAS
Volume 24, Number 9, September 2023
Pages: 4651-4660

ISSN: 1412-033X
E-ISSN: 2085-4722
DOI: 10.13057/biodiv/d240905

Isolation of euryhaline microalgal strains from tropical waters of Brunei Darussalam for potential biomass production

WARDINA ROSELI, YASUAKI TANAKA, HUSSEIN TAHA♥
Department of Environmental and Life Sciences, Faculty of Science, Universiti Brunei Darussalam. Jl. Tungku Link, Gadong BE1410, Brunei Darussalam. Tel.: +673-246-0923 ext 1372, ♥email: hussein.taha@ubd.edu.bn

Manuscript received: 18 July 2023. Revision accepted: 5 September 2023.

Abstract. *Roseli W, Tanaka Y, Taha H. 2023. Isolation of euryhaline microalgal strains from tropical waters of Brunei Darussalam for potential biomass production. Biodiversitas 24: 4651-4660.* Rapid urbanization has increased the accumulation of excess nitrogen (N) and phosphorus (P) in natural water bodies (eutrophication). Microalgae are seen as a viable candidate to resolve the problem due to their ability to absorb nutrients from the eutrophicated water (phycoremediation). Euryhaline microalgae could significantly benefit because they can tolerate various salinities while maintaining high biomass productivity. This study aimed to isolate euryhaline microalgae from tropical waters and evaluate the algae's potential to produce biomass and absorb nutrients in a wide range of salinities. Three strains labelled W1, W2, and W3 were isolated from Brunei waters and confirmed by DNA barcoding as *Desmodesmus* sp., *Micractinium* sp., and *Chlorococcum* sp., respectively. These strains were screened for salinity tolerance by exposing them to eight conditions (salinity 0, 5, 10, 15, 20, 25, 30, and 35) and evaluated for their high growth performance based on optical density. While the growth of *Desmodesmus* sp. and *Chlorococcum* sp. decreased from its highest value by 67% and 61%, respectively, the growth of *Micractinium* sp. was only reduced by 46%, and therefore, *Micractinium* sp. was considered to be the most euryhaline species and studied further in the next scale-up experiment. *Micractinium* sp. was cultivated at salinities of 0, 15, and 30 and recorded the highest biomass production of 54.1 ± 6.0 mg L^{-1} d^{-1} at salinity 15. Furthermore, they produced high amounts of N and P in their biomass, indicating that they are suitable for the phycoremediation of eutrophic water bodies. Therefore, *Micractinium* sp. is a potential candidate for open-pond cultivation because of its tolerance to a wide range of salinities and high biomass productivity.

Keywords: Biomass, euryhaline microalgae, eutrophication, phycoremediation, salinity

INTRODUCTION

Over the past few years, microalgae biomass has received much interest for various biotechnological applications due to its quick growth rate and robust vitality (Chen et al. 2018). The algal biomass can be applied for the production of high-value products, including chemicals (vitamins, pigments, antioxidants), oils (omega-3 fatty acids), protein, and animal feed (Coustets et al. 2015). It is a promising future energy resource as it can quickly grow, has high carbohydrate and lipid content, and is cultivated in saline and various types of wastewater with higher photosynthetic potential than all other terrestrial energy crop plants (Ren et al. 2014). Their photosynthetic mechanism resembles that of land-based plants. They have efficient access to water, CO_2, and other nutrients and are generally more efficient in processing solar energy into biomass (Asokaraja et al. 2011). In addition, microalgae can be grown using marine or wastewater, so they are not competing for the limited freshwater supply (Abomohra et al. 2016). Through *de novo* synthesis, biomass can be exploited to produce valuable resources and high-value compounds such as carbohydrates, proteins, and lipids (Rawat et al. 2013). The surge of anthropogenic activities as a result of expanding human population, industrialization, and urbanization has been a growing source of concern due to the excessive discharge of harmful wastes into natural water bodies, which degrades water quality and contaminates the whole water environment known as eutrophication (Ummalyma et al. 2018). Microalgae-based treatments, also known as phycoremediation, are deemed more efficient and safer for the environment when compared to physicochemical treatment technologies for wastewater (Malla et al. 2015). Phycoremediation is the utilization of macro- or microalgae to reduce or biotransform contaminants from wastewater, such as nutrients and hazardous compounds (Mulbry et al. 2008). Microalgae could also grow in industrial wastewater to remove contaminants and produce valuable bioproducts (Chen et al. 2018).

Screening for novel microalgal strains is crucial in improving the viability of biomass production and identifying potential producers. An essential first step is the selection of strains that consider the later phases in processing, such as their resilience, simple and inexpensive downstream processing, and the efficient production of biorefinery (Pereira et al. 2016). To withstand broad environmental conditions and outgrow competitors and predators, microalgae intended for large-scale development must be durable and present at high growth rates. Euryhaline microalgal strains present a significant benefit for large-scale production in open ponds. They can tolerate a broad range of salinities, even when the salinities in the culture medium fluctuate and may contain impurities. Yet, these algae can outgrow and have no consequence on biomass productivity (Pereira et al. 2016). Using seawater

or brackish water to cultivate cyanobacteria and microalgae reduces reliance on freshwater resources (Abomohra et al. 2016). Large quantities of water are required to mass-cultivate microalgae, such as biofuels (Borowitzka and Moheimani 2013). This is especially concerning in tropical areas, where high evaporation rates throughout the year can lead to concerns of increased salinity (von Alvensleben et al. 2016).

Microalgal strains with a wide salinity tolerance are particularly desirable for long-term cultivation in seawater that is both effective and sustainable (Borowitzka and Moheimani 2013). Salinity is a stress that impacts a variety of physiological and biochemical pathways involved in microalgae development and growth (Chokshi et al. 2017). Most microalgae can tolerate salinity fluctuations through the K+/Na+ pump and through the production of osmolytes (e.g., glycine betaine, proline, sucrose, glycerol), which contributes to the osmotic ability of cell turgor and volume control while the latter to protect and restore damaged proteins, nucleic acids and membrane (von Alvensleben et al. 2013). Ionic, osmotic, and oxidative salt stress are the three main ionic stress types resulting from an ion homeostasis imbalance. High salt in the surrounding environment decreases the osmotic potential and reduces water absorption (Chokshi et al. 2017). Reactive oxygen species (ROS) production is imbalanced during oxidative stress caused by salt stress (Affenzeller et al. 2009). Various ROS were produced in microalgae cells under unfavorable conditions such as salinity stress, and these ROS damaged cellular macromolecules such as protein, lipids, and DNA. Then, cell growth was disrupted (Yun et al. 2019). Algae have numerous natural protective mechanisms, including antioxidant enzymes (e.g., APX), proline, non-enzymatic molecules, etc., to protect against cell damage caused by ROS (Chokshi et al. 2015). The preferred storage products in varying stress conditions are lipids and carbohydrates, which can be used by the cells for their survival during unfavourable situations (Chokshi et al. 2015).

This research aimed to isolate euryhaline microalgal strains from Brunei waters and evaluate the algae's potential for commercial applications such as biofuel, biofertilizer, and bioremediation of wastewater. The objectives of this research were (1) to isolate microalgal strains from fresh, brackish, and marine waters in Brunei, (2) to screen euryhaline strains by conducting laboratory experiments on salinity tolerance, and (3) to evaluate biomass production for selected algal strains in scale-up experiments.

MATERIALS AND METHODS

Isolation of microalgal strains

Microalgal strains were sampled at Wasan Paddy Field, Brunei (4.784N, 114.820E) by scooping the surface water of the flooded paddy field in December 2019. BG11 medium (Allen 1968) enriched the water sample. After at least 3 weeks of enhancing the algal growth in controlled conditions of 12 hours of exposure to approximately 80 μmol m^{-2} s^{-1} light intensity as well as the temperature of 25 ± 1°C, the culture was purified by repeated streaking on BG11 agar plates until pure colonies were observed (Andersen 2005). Colonies obtained through repeated streaking were transferred using a sterile loop from the agar plates into liquid BG11 medium for further growth. The plates and liquid cultures were kept at 80 μmol m^{-2} s^{-1} on a 12:12 hour light-dark cycle at 25 ± 1°C.

Identification of microalgal strains

The strain was identified microscopically using a light microscope with 100x magnification (Olympus CH30). DNA barcoding was used to further identify the microalgal strains up to the genus level. Each algal strain was harvested in sterile 2 mL centrifuge tubes during the exponential growth phase (day 4). Afterward, the tubes were centrifuged at 3500 rpm for 10 minutes to extract 25 to 30 mg of algal cell pellets. These cell pellets were frozen until they could be analyzed further. Total genomic DNA was extracted using Qiagen's DNeasy® blood and tissue kit, and the procedure was carried out according to the manufacturer's instructions. NanoDrop 2000 spectrophotometer (Thermo Scientific™) was used to measure the concentration of DNA. A service provider carried out DNA barcoding. The DNA samples were barcoded using the 18S rRNA gene. The resulting 18S rRNA gene sequences were uploaded to the GenBank database with accession no. ON352774 to ON352776, compared for percent similarity with all the sequences in the GenBank database by using the Basic Local Alignment Search Tool (BLAST). For tree construction, the top ten BLAST hits were selected for each sample. MEGA11 (Tamura et al. 2021) was used to align sequences via ClustalW and to construct an unrooted neighbor-joining tree with p-distance. Bootstrapping was also carried out using 1,000 replicates.

Screening experiments for euryhaline microalgae

Experimental procedure

Salinities (0, 5, 10, 15, 20, 25, 30, and 35) were prepared for the culture media by mixing filtered and sterilized seawater collected at Tanjung Batu Beach, Brunei Darussalam (5.041N, 115.061E) in September 2020 with distilled water. Salinity was measured with YSI 556 using the Practical Salinity Scale. Each bottle was filled with 40 mL of algae concentrate and 160 mL of BG11 media (total volume = 200 mL), and four replicates were made for each salinity. For 14 days, the cultures were lit at 100 μmol m^{-2} s^{-1} with a 12:12 hour light-dark cycle. A water bath with a submersible heat rod was used to keep the temperature at 25 ± 1°C.

Calculations of growth rate constant and reduction percentage

On days 0, 2, 4, 7, 10, and 14, the optical density of the culture water was measured to monitor algal growth. A spectrophotometer (Shimadzu UV-1800) was used to measure the absorbance at 750 nm in a portion (5 mL) of the culture water on respective days (Griffiths et al. 2011; Jia et al. 2015).

The growth rate is essential in finding suitable microalgal strains for biomass production. A growth rate constant was calculated from the absorbance as follows (Eq. 1):

$$\text{Growth rate constant } \left(\mu \text{ day}^{-1}\right) = \frac{\ln\left(\frac{A_2}{A_0}\right)}{T_2 - T_0} \quad (1)$$

Where A_0 is absorbance measured on day 0, A_2 is absorbance measured on day 2, T_0 is day 0, and T_2 is day 2. The growth rate constant was calculated only for the first two days because the growth rate was the fastest during this period.

Furthermore, to evaluate the tolerance of algae to a wide range of salinities, a reduction percentage was calculated using Eq. 2.:

$$\text{Reduction percentage } (\%) = \frac{B_{max} - B_{min}}{B_{max}} \times 100 \quad (2)$$

Where B_{max} is the maximum mean absorbance and B_{min} is the minimum mean absorbance.

Scale-up experiments

Experimental procedure

The selected microalgal strain from the screening experiments was used for the scale-up experiment based on the reduction percentage of growth and average absorbance for all salinities on the final day of the experiment. Three ranges of salinities were selected based on absorbance from previous screening experiments. The salinities were prepared for the culture media using filtered and sterilized natural seawater collected offshore Muara Beach, Brunei (5.050N, 115.096E) from a boat in June 2021. For the culture, 2 L clear bottles (n= 3) were used, and each bottle contained 400 mL of algae concentrate with 1600 mL BG11 medium. The cultures were illuminated under 100 µmol m^{-2} s^{-1} in a cycle of 12 hours of light and 12 hours of darkness. Aeration was provided using air stones. The temperature was kept at 28 ± 1°C by submerging the culture bottles in a water bath with a submergible heat rod for 7 days.

Analysis and calculations of biomass

After 7 days of cultivation, a portion of the culture water was filtered through pre-combusted and pre-weighed glass microfiber filter paper with a diameter of 47 mm and pore size of 0.7 µm (Whatman GF/F). After completely filtering the cultures, the filter papers were rinsed with distilled water to remove salts and transferred to a sterile petri dish using clean forceps. Then, these filter papers were dried in an oven with circulating air at 50°C for at least 5 hours. Once dried, the filters were cooled to room temperature, and the dry weight was measured using an analytical balance with a precision of 0.1 mg.

The dry weight of the algal biomass was calculated by subtracting the final weight of the filter with attached microalgal cells with the pre-weighed mass of the filter.

Daily biomass production was calculated based on Eq. (3):

$$\text{Biomass production } \left(\text{mg L}^{-1}\text{ d}^{-1}\right) = \frac{DBW_f - DBW_i}{t} \quad (3)$$

Where DBW_f is the final dry biomass weight in mg L^{-1}, DBW_i is the initial dry biomass weight in mg $L^{-1,}$ and t is the cultivation time in days.

Analysis and calculations of nitrogen and phosphorus content

The dried filter papers with the retained microalgal cells were used to determine nitrogen content (Collos et al. 1999) and phosphorus content (Hansen and Koroleff 1999) in the cultured microalgae.

Total nitrogen (N) and phosphorus (P) content in a whole filter sample were obtained from the N and P content in each disc (diameter 6 mm), and the ratio of N and P content (mg) to total biomass (mg) were calculated (N% and P%, respectively).

N and P in the culture (µg L^{-1}) were measured by dividing the N and P content (µg) with the volume of filtered culture (L). Algal N and P production rates were calculated by the Eq. (4):

$$\text{N and P production } \left(\mu\text{g L}^{-1}\text{ d}^{-1}\right) = \frac{B_f - B_i}{t} \quad (4)$$

Where B_f is the final N and P in culture on the final day of the experiment, B_i is the initial N and P in culture, and *t* is the total days of the experiment.

Analysis and calculations of chlorophyll pigments

10 mL of culture was taken into a centrifuge tube (15 mL) for photosynthetic pigment analysis. The samples were centrifuged for 10 minutes at 3,500 RPM, and the supernatant was removed. Algal pellets were immersed in 5 mL of 90% acetone and maintained in the freezer until needed. Chlorophyll (Chl) pigments were measured using the method Ritchie (2006) described with modifications.

The equations for Chl a (Eq. 5a) and b (Eq. 5b) content in microalgal cells are shown:

$$\text{Chl } a \left(\mu\text{g mL}^{-1}\right) = 11.8668 \times A_{664} - 1.7858 \times A_{647} \quad (5a)$$

$$\text{Chl } b \left(\mu\text{g mL}^{-1}\right) = 4.8950 \times A_{664} - 18.9775 \times A_{647} \quad (5b)$$

Where A_{664} is absorbance measured at 664 nm, and A_{647} is measured at 647 nm. Therefore, the daily Chl production can be calculated by Eq. 6:

$$\text{Chl production } \left(\mu\text{g L}^{-1}\text{ d}^{-1}\right) = \frac{C_f - C_i}{t} \quad (6)$$

Where C_f indicates the final chlorophyll in the culture on the last day of the experiment, C_i represents the initial chlorophyll in the culture, and *t* is the total number of experiment days.

Statistical analysis

The data in this study was presented as mean ± SD. One-way analysis of variance (ANOVA) was used to examine differences between treatments in biomass production, N:P ratio, N% and P%, and N and P production. When the results of ANOVA were significant, the Tukey HSD test was used to see if there was a specific difference between treatments. JMP software (SAS Institute, USA) was used for statistical analysis. Throughout this study, a significant level of $p < 0.05$ was applied.

RESULTS AND DISCUSSION

Isolation and identification of microalgal strains

The isolated microalgae showed different morphological features (Table 1). The amplified 18S rRNA gene sequences of three isolated microalgal strains W1, W2, and W3, matched closely with *Desmodesmus* sp. *Micractinium* sp., and *Chlorococcum* sp., respectively (Table 1). Sequence-based phylogenetic analysis supported and confirmed identifying the three isolated microalgal strains (Figure 1).

Screening experiments for euryhaline microalgae

Microalgae growth curve

The effect of different salinities on the algal growth of three strains (*Desmodesmus* sp., *Micractinium* sp., and *Chlorococcum* sp.) are shown in Figure 2. These graphs show growth curves of the strains in 14 days of culture period and show that all three strains were growing gradually in all the salinity ranges in this experiment. The initial absorbance was 0.0104 (Figure 2A), 0.0174 (Figure 2B) and 0.0098 (Figure 2C) for *Desmodesmus* sp. *Micractinium* sp. and *Chlorococcum* sp. respectively.

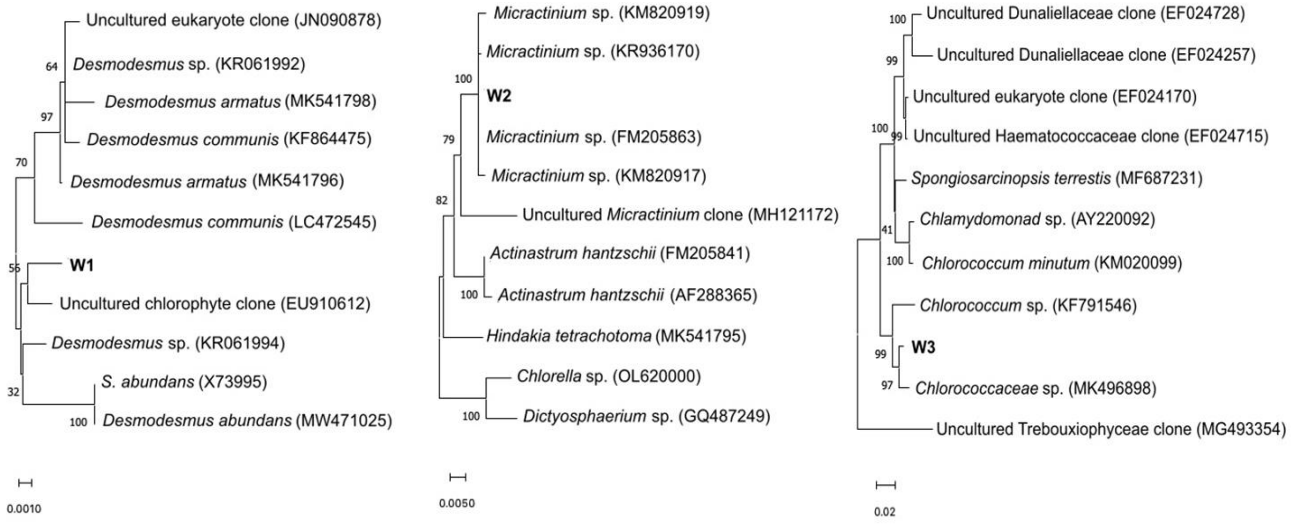

A **B** **C**

Figure 1. Phylogenetic trees of the isolates: A. W1, B. W2, and C. W3, and the top ten BLAST hits of the GenBank sequences

Table 1. The identifications, top BLAST hits, similarities between the amplified sequences of three microalgal strains, and closest relative sequences with the morphological characteristics viewed under 100x magnification

Strain codes	Species identification	Top BLAST hit and GenBank accession number	Identity (%)	Microscopic observation	Microscopic image
W1	*Desmodesmus* sp.	*Desmodesmus* sp. KR061994	99.49	Green algae, spines present, round cells, cells arranged in rows of 2,4,8 and 10	
W2	*Micractinium* sp.	*Micractinium* sp. FM205863	100	Green algae, unicellular, flagella not seen, round cells	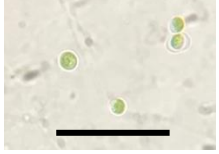
W3	*Chlorococcum* sp.	Chlorococcaceae sp. MK496898 *Chlorococcum* sp. KF791546	98.24 96.08	Green algae, unicellular, round cells, cells form irregular clumps form moist films around cells	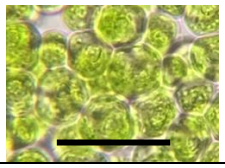

Growth rate constant from day 0 to day 2

Growth rate constants were calculated for all strains from the absorbance measured from day 0 to day 2 (Figure 3). Both *Desmodesmus* sp. and *Micractinium* sp. had their optimum salinity at 5 with the growth constant of 0.592 ± 0.017 day^{-1} and 0.464 ± 0.019 day^{-1}, respectively (Figure 3.A and 3.B). *Chlorococcum* sp. had its optimum salinity at 15 with the growth constant of 0.576 ± 0.015 day^{-1} (Figure 3.C). There was a significant difference in growth rate constants between the most optimum and least optimum salinities. *Micractinium* sp. was most tolerant to the wide range of salinities among the three strains, considering that the growth rate constant decreased only by 25% from the salinity 5 to 30 (Figure 3.B).

Microalgae biomass on day 14

Figure 4 shows the absorbance measured on day 14 for all microalgal strains. The highest absorbance for *Desmodesmus* sp. was 0.073 ± 0.003 at salinity 10. It decreased by 67% at salinity 25 (Figure 4.A), and *Micractinium* sp. had the highest absorbance at salinity 30 with 0.121 ± 0.004 and decreased by 46% at salinity 0 (Figure 4.B). In comparison, *Chlorococcum* sp. had the highest absorbance at salinity 20 with absorbance of 0.083 ± 0.004 (Figure 4.C) and reduced by 61% at salinity 0. These reduction percentages showed the ability of the strain to tolerate the range of salinities; *Micractinium* sp. was more tolerant than *Desmodesmus* sp. and *Chlorococcum* sp.

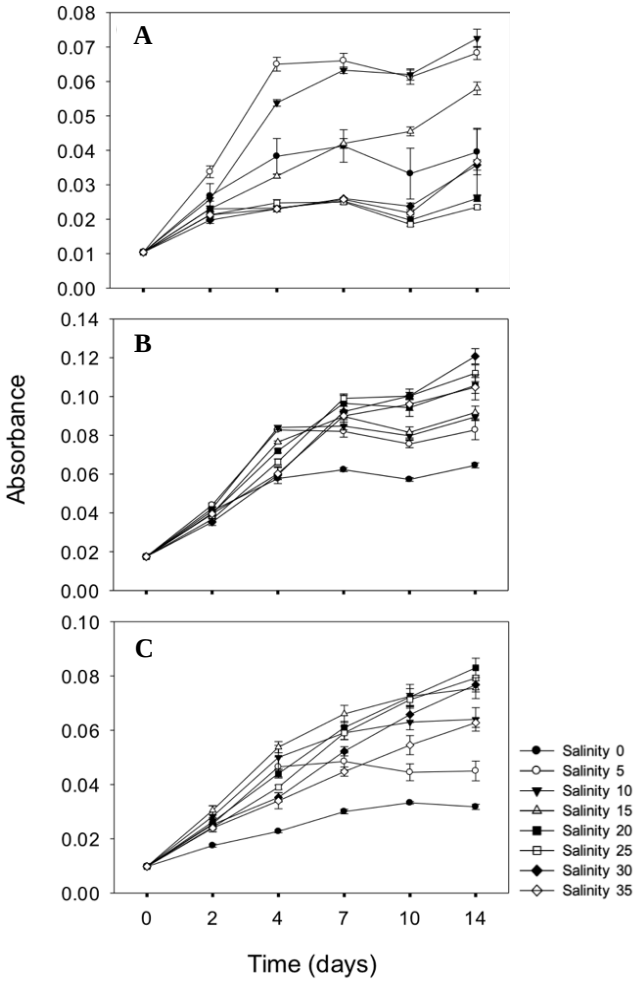

Figure 2. Comparison of growth of three microalgal strains: A. *Desmodesmus* sp., B. *Micractinium* sp., and C. *Chlorococcum* sp. with eight different salinities (salinity 0, 5, 10, 15, 20, 25, 30, 35) for 14 days. Data are expressed as mean ± SD of 5 replicates

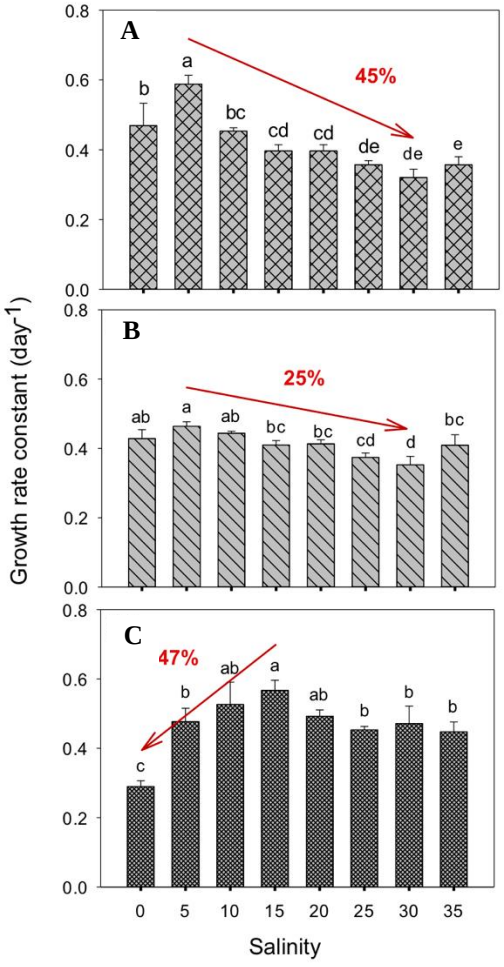

Figure 3. Growth rate constant from day 0 to day 2 for three microalgal strains: A. *Desmodesmus* sp., B. *Micractinium* sp., and C. *Chlorococcum* sp. under eight different salinities. Different letters on bar graphs indicate significant differences among salinities. Red arrows show the reduction percentage from most optimum to least optimum salinity

Average biomass for all salinities on day 14

The average absorbance on day 14 for all salinity treatments showed a significant difference between the three strains (Figure 5). The average absorbance of *Micractinium* sp. was highest at 0.096 ± 0.017, and its growth was more efficient than *Desmodesmus* sp. and *Chlorococcum* sp., which had lower absorbance of 0.045 ± 0.018 and 0.065 ± 0.017, respectively. This means salinity tolerance and biomass production were different in different microalgal strains. *Micractinium* sp. favoured higher salinities around 25 to 30. Therefore, this strain was used for the scale-up experiment.

Scale-up experiments for *Micractinium* sp.

Analysis of biomass, nitrogen and phosphorus content, and chlorophyll pigments

The highest biomass production was 54.11 ± 5.97 mg L^{-1} d^{-1} at salinity 15, and the lowest was 26.89 ± 2.73 mg L^{-1} d^{-1} at salinity 30 (Figure 6.A). There was no significant difference in biomass production between salinity 0 and 30. The highest N and P production was at salinity 15 with 1,103.57 ± 191.94 µg L^{-1} d^{-1} and 502.48 ± 124.94 µg L^{-1} d^{-1}, respectively (Figure 6.B and 6.C). There was a significant difference between the highest and lowest of N and P production. N% was highest at salinity 0 with 3.01 ± 0.43%, and there were no significant differences between salinity 15 and salinity 30 (Figure 6.D). While P% was highest at salinity 30 with 1.34 ± 0.40%, no significant differences existed between salinity 0, 15, and 30 (Figure 6.E). The lowest molar N:P ratio was 3.65 ± 0.65 at salinity 30 (Figure 6.F). There was no significant difference between salinity 30 and salinity 15, but the highest N:P ratio with 8.74 ± 4.10 at salinity 0 was significantly different. Chlorophyll *a* production was the highest at salinity 15 with 2051.75 ± 337.62 µg L^{-1} d^{-1}, and there was a significant difference with the lowest production at salinity 0 with 1301.76 ± 465 µg L^{-1} d^{-1} (Figure 6.G). The highest chlorophyll *a*/biomass was at salinity 30 with 0.06 ± 0.01 and the lowest at 0.04 ± 0.004 for salinity 15 (Figure 6.H). There was a significant difference between the highest and lowest chlorophyll *a*/biomass.

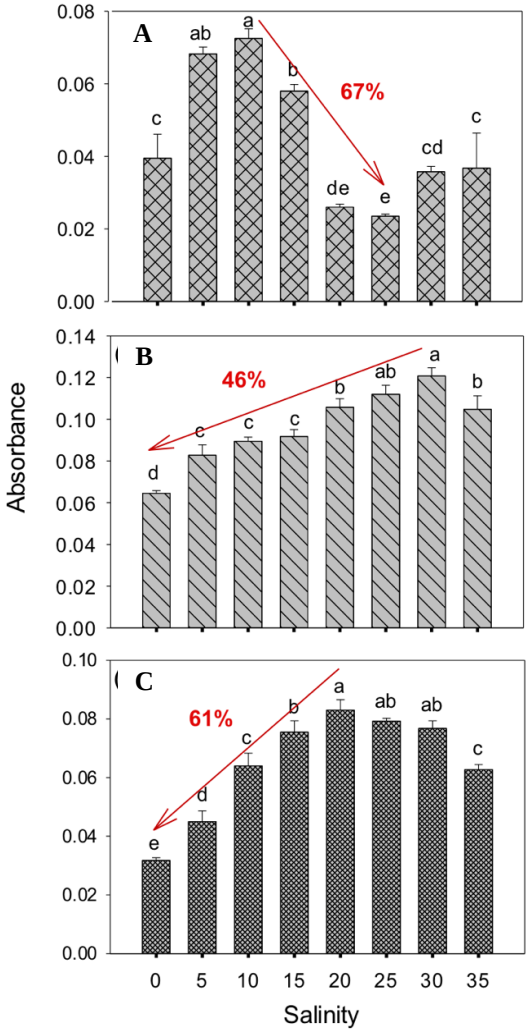

Figure 4. Absorbances were measured on day 14 for three microalgal strains: (A) *Desmodesmus* sp., (B) *Micractinium* sp., and (C) *Chlorococcum* sp. at different salinities. Different letters on bar graphs indicate significant differences among salinities. The red arrows show the reduction percentage from the most optimum to the least optimum salinity

Discussion

Isolation and identification of microalgal strains

Microscopic morphological observations for the W1 strain exhibited 2, 4, 8, and 10-cell colonies, with 4-cell colonies being the most common. This was most apparent when there was no stress, such as salinity (Pozzobon et al. 2020). The long spines visible under the oil-immersion lens at the first and last cells of the colony were the most distinguishing morphology for this strain. Despite being similar to *Scenedesmus* sp., the cells for this strain were rounder. Considering these morphological characteristics, this strain was predicted to be *Desmodesmus* sp. This morphological identification was confirmed by DNA barcoding. This strain has previously been studied for biomass production, such as biofuel and nutraceutical applications (Pozzobon et al. 2020) and treating wastewater (Samorì et al. 2013).

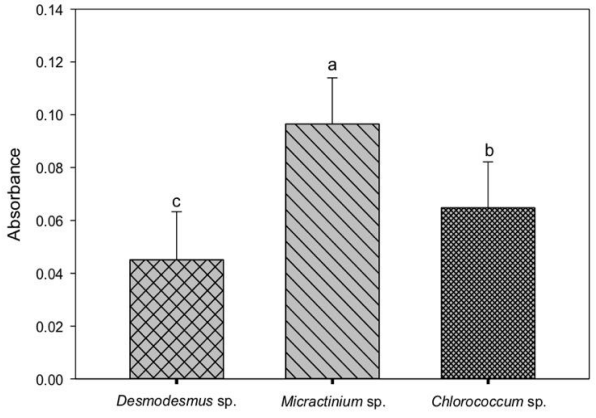

Figure 5. Average absorbance for all salinities on day 14 for all three microalgal strains. Different letters on bar graphs indicate significant differences between strains

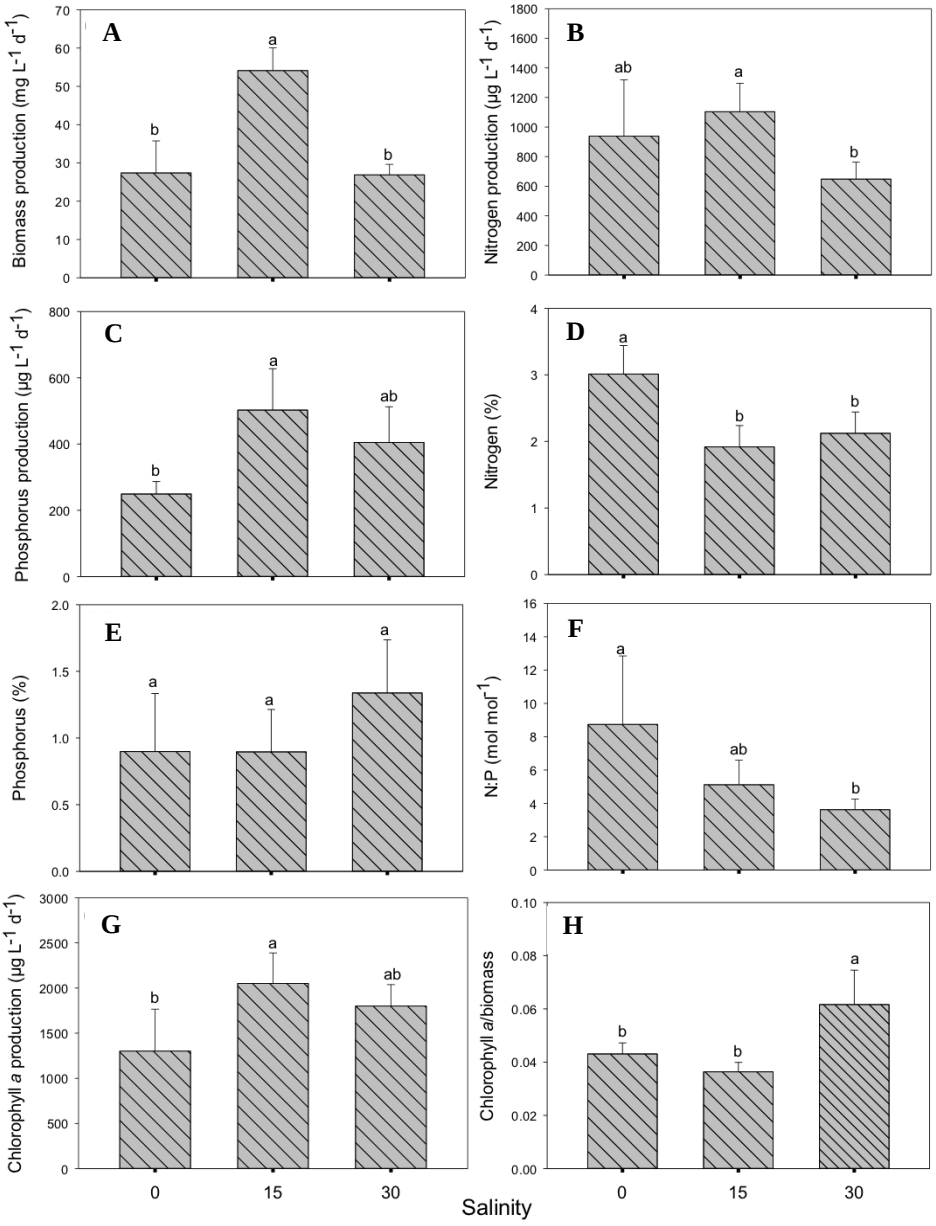

Figure 6. Effect of three different salinities (salinity 0, 15, and 30) on: A. Biomass production, B. N production, C. P production, D. N%, E. P%, F. N:P ratio, G. chlorophyll *a* production and H. Chlorophyll *a*/biomass for *Micractinium* sp. Different letters on bars indicate significant differences among treatments. Data are expressed as mean ± SD of 5 replicates

The cells of the W2 strain were spherical in shape, lacked flagella, and had a chloroplast that occupied nearly the whole cellular cavity, suggesting that they are *Chlorella* sp. However, this strain was identified as *Micractinium* sp. by DNA barcoding. Each cell has a diameter ranging from 3 to 9 µm (Chae et al. 2019)**.** Similar to *Chlorella* sp. morphologically and belonging to the same family, Chlorellaceae, *Micractinium* sp. has been actively studied for biodiesel production, high-value chemicals, for its ability to produce high-cell density cultivation and high lipid production (Liu et al. 2021).

The W3 strain was predicted to be *Chlorococcum* sp. based on its morphological characteristics, as when observed under the microscope, the cells were unicellular and non-motile, each with a parietal cup-shaped chloroplast. The nucleus was about in the center of the cell and had a thicker cell wall. No flagella was observed on the cells, and they were clustered together. DNA barcoding confirmed that the W3 strain was *Chlorococcum* sp., previously used in biomass production for biodiesel (Kirrolia et al. 2012) and bioremediation (Singh and Ummalyma 2020).

Screening experiments for euryhaline microalgae

Water availability and salinity are crucial factors for the sustainability of large-scale microalgae cultivation. This is especially concerning in tropical areas, where high precipitation and evaporation rates can lead to fluctuation

in salinity all year round. To screen for euryhaline microalgae, three strains, namely *Desmodesmus* sp. *Micractinium* sp and *Chlorococcum* sp. were cultured in a wide range of salinity in the second experiment, and all microalgal strains grew well and exhibited an exponential growth phase from day 0 to day 2 (Figure 2). There was no noticeable lag phase for all of the strains. Still, they all started to grow immediately, indicating that they could adapt to various salinities without any more acclimation. Whereas the precise mechanisms behind the strains' lack of a lag phase remained unknown, other researchers found similar results (Luo et al. 2016; Deng et al. 2017).

Enzymes are generally inactivated under high salinity conditions for freshwater microalgae, reducing the photosynthetic rate (von Alvensleben et al. 2016). Also, the imbalance of ions in the cells causes water loss from the cells (Erdmann and Hagemann 2001). The effectiveness and sustainability of long-term microalgae cultivation in saline water are widely preferred for microalgal strains capable of tolerating a wide range of salinity. Because *Desmodesmus* sp. *Micractinium* sp. and *Chlorococcum* sp. were isolated from freshwater environments; it was expected that they would be unable to withstand the presence of salt. However, the present experiments revealed that all three species were tolerant to the high salinity, as seen by the low reduction percentage (Figure 3). *Micractinium* sp. had the lowest reduction percentage, which was considered to be the most euryhaline. *Desmodesmus communis* has a high salt tolerance, which has been reported by other research studies (von Alvensleben et al. 2016; Sahle-Demessie et al. 2019). Previous studies demonstrated that *Micractinium* sp. could grow to various salinities (Adar et al. 2016) and *Chlorococcum humicola* (Singh et al. 2018).

On day 14, the average absorbance of *Micractinium* sp. was higher than the other two strains when all salinity ranges were considered (Figure 5). *Micractinium* sp. could potentially tolerate a wide range of salinities by hardening their cells when exposed to high salinities (Adar et al. 2016). Considering a large-scale and industrial production of microalgae, *Micractinium* sp. would be beneficial when biomass production facilities are located near the downstream environment (e.g., close to the sea) because the salinity of the water is maintained relatively high. Therefore, the strain *Micractinium* sp. was focused on in the next scale-up experiment.

Scale-up experiment for Micractinium *sp.*

The ability of strain *Micractinium* sp. to grow in a greater salinity range was demonstrated in the third experiment of this study, proving its euryhaline physiology. Salinity is a complex stress that affects various physiological and biochemical pathways involved in microalgae development and growth. Under laboratory conditions, the optimum salinity for *Micractinium* sp. to yield high biomass productivity was 15 (Figure 6.A).

A study by Adar et al. (2016) reported that *Micractinium* sp. grew best at salinities from 1.8 ppt until 18.3 ppt, which agreed with current research. The Chlorellaceae family, which comprises *Micractinium* sp., is morphologically similar to that of *Chlorella* sp. The latter had been widely studied previously for its tolerance to salinities. A previous study reported that the growth of *Chlorella capsulata* was highest at a salinity of 25 (Ebrahimi and Salarzadeh 2016), and another study by Anandraj et al. (2020) found that *Chlorella* sp. acclimatized best at a salinity of 20. While this study produced the most biomass at the optimum salinity, *Micractinium* sp. continued to grow at the highest salinity despite producing slightly lesser biomass. High salinity hinders algal osmoregulation, preventing them from absorbing water and nutrients, limiting growth, and possibly resulting in death. Salinity stress is often associated with an over-production of reactive oxygen species (ROS), which can damage cellular macromolecules, including protein, lipid, and DNA, which restricts cell growth, leading to decreased biomass. Other studies have previously shown similar findings of reducing biomass productivity with a rise in NaCl concentration for *Chlorella* sp. (Pandit et al. 2017; Trivedi et al. 2019). This could also be attributed to the cost of energy of maintaining osmotic balance in a high-saline environment being greater than the energy of growth and cell division.

Nitrogen (N) is an important component for microalgal growth since it is required for the formation of proteins, peptides, enzymes, genetic materials, chlorophyll molecules, and energy transfer molecules like ADP and ATP (Deng et al. 2017; Chai et al. 2021). Phosphorus (P) is a macronutrient that regulates cell growth and metabolism, particularly in cells that are involved in photosynthetic activity (Liang et al. 2013). At their respective optimal salinities, N and P production by *Micractinium* sp. increased with increased biomass production (Figure 6.B and C). This is due to the fast growth rate of *Micractinium* sp., which resulted in rapid nutrient uptake. Nutrient uptake into the algal cells is the primary mechanism for nutrient removal from wastewater.

The highest biomass had the lowest N% and P% according to the findings of this study (Figure 6.D and E). N needs to be used for cell division and growth of microalgae because it is a component of protein synthesis. The amount of nitrogen in the culture medium was sufficient to sustain a metabolic balance between carbon fixation and nitrogen assimilation, which is required for cellular metabolism (Adams et al. 2013). P% was also lower at high biomass, possibly due to the phosphate essential for growth being absorbed by the algal cells. In comparison, N% and P% increased for *Micractinium* sp. at high salinity. According to Rees et al. (1980), the nitrate transport rate was high and correlated with the salt concentration in the media. The present results of N% and P% showed that the proportion of carbohydrates in the algal cells increased when biomass production increased under suitable salinity conditions, which led to lower N% and P%, and the proportion of proteins increased when biomass production decreased under unfavorable salinity conditions, which led to higher N% and P%. The N:P ratio was reduced at the greatest biomass production with 5.12 ± 1.47 (Figure 6.F), indicating that they are N limiting because the ratios were lower than the Redfield ratio

(16:1). The Redfield ratio is a term used to describe the ideal N:P ratio for microalgae (Klausmeier et al. 2004). As N availability decreases, overall protein content decreases, causing the N:P ratio of the cells to decrease over time.

Chlorophyll pigment was measured on the first and last days of the experiment on three different salinity ranges to examine the effect of salinity on the photosynthetic process of *Micractinium* sp. Chlorophyll is a green pigment found in photosynthetic organisms like microalgae. It absorbs and transfers light energy, which is essential for photosynthesis (Li and Chen 2015). Plants and microalgae commonly respond to stress by reducing photosynthetic pigments like Chlorophyll-*a* (Chl-*a*) (Pancha et al. 2015). Chl-*a* production was reduced at 1,800 ± 237 µg L^{-1} d^{-1} (Figure 6G) at the highest salinity investigated in this study for *Micractinium* sp. at salinity 30. The decline was attributable to a decrease in photosynthetic rate due to osmotic and toxic stress from salt (Kirrolia et al. 2012; Chokshi et al. 2017). During salt stress, algal cells produce more reactive oxygen species (ROS), which reduces photosynthetic efficiency by peroxidation of thylakoid lipids and degrading the PS II complex (Liu et al. 2012). However, the ratio of Chl-*a*/biomass of *Micractinium* sp. increased at the salinity 30 (Figure 6.H). This might be related to reduced PS II activity and an indirect sign of salinity stress. High Chl-*a*/biomass ratios also suggest that the antenna size is shrinking, which could play a protective role against photooxidative damage. Under high salinity stress, Pal et al. (2011) and Pancha et al. (2015) found comparable trends in high Chl-*a*/b or carotenoids/total Chl in *Scenedesmus* sp. and *Nannochloropsis* sp. respectively.

In summary, three strains were successfully isolated from Brunei waters at Wasan Paddy Field, Brunei Darussalam, as W1, W2, and W3. The W1, W2, and W3 morphologies supported and confirmed by DNA identification that these strains were *Desmodesmus* sp. *Micractinium* sp. and *Chlorococcum* sp. respectively. All three strains were screened under a salinity variation (salinity 0, 5, 10, 15, 20, 25, 30, and 35) by analyzing their growth throughout the experiment. Based on the reduction percentage for biomass production, it was determined that *Micractinium* sp. was the most euryhaline strain. Therefore, *Micractinium* sp. was selected for further analyses. It was found that it had a specific optimum salinity of 15 in this study. The highest growth was observed at this optimum salinity, and the strain produced high N and P. Also, N% and P% were reduced, indicating that the strain successfully used up these nutrients for growth while increasing carbohydrate content, which is beneficial for the dual purposes of wastewater remediation and biomass production. Other environmental factors that may affect the growth and biochemical composition of the strain should be investigated further. Due to the rapid growth of *Micractinium* sp. it was considered a promising candidate for biomass production. It can be considered an appropriate strain for open-pond microalgal cultivation in the presence of salinity. Aside from that, this strain has the potential to be studied further in terms of lipid production, antioxidant capabilities, and antimicrobial characteristics, enabling its prospective benefits to be completely explored.

ACKNOWLEDGEMENTS

Universiti Brunei Darussalam funded the research project.

REFERENCES

Abomohra AE, Jin W, Tu R, Han S, Eid M, Eladel H. 2016. Microalgal biomass production as a sustainable feedstock for biodiesel: current status and perspectives. Renew Sustain Energy Rev 64: 596-606. DOI: 10.1016/j.rser.2016.06.056.

Adams C, Godfrey V, Wahlen B, Seefeldt L, Bugbee B. 2013. Understanding precision nitrogen stress to optimize the growth and lipid content tradeoff in oleaginous green microalgae. Bioresour Technol 131: 188-194. DOI: 10.1016/j.biortech.2012.12.143.

Adar O, Kaplan-Levy RN, Banet G. 2016. High temperature Chlorellaceae (Chlorophyta) strains from the Syrian-African Rift Valley: the effect of salinity and temperature on growth, morphology and sporulation mode. Eur J Phycol 51 (4): 387-400. DOI: 10.1080/09670262.2016.1193772.

Affenzeller MJ, Darehshouri A, Andosch A, Lütz C, Lütz-Meindl U. 2009. Salt stress-induced cell death in the unicellular green alga *Micrasterias denticulata*. J Exp Bot 60 (3): 939-954. DOI: 10.1093/jxb/ern348.

Allen MM. 1968. Simple conditions for growth of unicellular blue-green algae on plates. J Phycol 4 (1): 1-4. DOI: 10.1111/j.1529-8817.1968.tb04667.x.

Anandraj A, White S, Naidoo D, Mutanda T. 2020. Monitoring the acclimatization of a *Chlorella* sp. from freshwater to hypersalinity using photosynthetic parameters of pulse amplitude modulated fluorometry. Bioresour Technol 309: 123380. DOI: 10.1016/j.biortech.2020.123380.

Andersen RA. (Ed.). 2005. Algal Culturing Techniques. Elservier, NY.

Asokaraja I, Mubarakali D, Ramasamy P, Bakdev E, Thajuddin N. 2011. Optimization of various growth media to freshwater microalgae for biomass production. Biotechnology (Faisalabad) 10 (6): 540-545. DOI: 10.3923/biotech.2011.540.545.

Borowitzka MA, Moheimani NR. 2013. Sustainable biofuels from algae. Mitigation Adaptation Strategies Glob Change 18: 13-25. DOI: 10.1007/s11027-010-9271-9.

Chae H, Lim S, Kim HS, Choi HG, Kim JH. 2019. Morphology and phylogenetic relationships of *Micractinium* (Chlorellaceae, Trebouxiophyceae) taxa, including three new species from Antarctica. Algae 34 (4): 267-275. DOI: 10.4490/algae.2019.34.10.15.

Chai WS, Tan WG, Halimatul Munawaroh HS, Gupta VK, Ho SH, Show PL. 2021. Multifaceted roles of microalgae in the application of wastewater biotreatment: a review. Environ Pollut 269: 116236. DOI: 10.1016/j.envpol.2020.116236.

Chen J, Li J, Dong W, Zhang X, Tyagi RD, Drogui P, Surampalli RY. 2018. The potential of microalgae in biodiesel production. Renew Sustain Energy Rev 90: 336-346. DOI: 10.1016/j.rser.2018.03.073.

Chokshi K, Pancha I, Ghosh A, Mishra S. 2017. Salinity induced oxidative stress alters the physiological responses and improves the biofuel potential of green microalgae *Acutodesmus dimorphus*. Bioresour Technol 244: 1376-1383. DOI: 10.1016/j.biortech.2017.05.003.

Chokshi K, Pancha I, Trivedi K, George B, Maurya R, Ghosh A, Mishra S. 2015. Biofuel potential of the newly isolated microalgae *Acutodesmus dimorphus* under temperature induced oxidative stress conditions. Bioresour Technol 180: 162-171. DOI: 10.1016/j.biortech.2014.12.102.

Collos Y, Mornet F, Sciandra A, Waser N, Larson A, Harrison PJ. 1999. An optical method for the rapid measurement of micromolar concentrations of nitrate in marine phytoplankton cultures. J Appl Phycol 11: 179-184. DOI: 10.1023/A:1008046023487.

Coustets M, Joubert-Durigneux V, Hérault J, Schoefs B, Blanckaert V, Garnier JP, Teissié J. 2015. Optimization of protein electroextraction from microalgae by a flow process. Bioelectrochemistry 103: 74-81. DOI: 10.1016/j.bioelechem.2014.08.022.

Deng XY, Gao K, Zhang RC, Addy M, Lu Q, Ren HY, Chen P, Liu YH, Ruan R. 2017. Growing *Chlorella vulgaris* on thermophilic anaerobic digestion swine manure for nutrient removal and biomass production.

Bioresour Technol 243: 417-425. DOI: 10.1016/j.biortech.2017.06.141.
Ebrahimi E, Salarzadeh A. 2016. The effect of temperature and salinity on the growth of *Skeletonema costatum* and *Chlorella capsulata* in vitro. Intl J Life Sci 10 (1): 40-44. DOI: 10.3126/ijls.v10i1.14508.
Erdmann N, Hagemann M. 2001. Salt acclimation of algae and cyanobacteria: a comparison. In: Rai LC, Gaur JP (eds.) Algal Adaptation to Environmental Stresses. Springer, Berlin, Heidelberg. DOI: 10.1007/978-3-642-59491-5_11.
Griffiths MJ, Garcin C, van Hille RP, Harrison STL. 2011. Interference by pigment in the estimation of microalgal biomass concentration by optical density. J Microbiol Methods 85: 119-123. DOI: 10.1016/j.mimet.2011.02.005.
Hansen HP, Koroleff F. 1999. Determination of nutrients. In: Grasshoff K, Kremling K, Ehrhardt M. Methods of Seawater Analysis (3rd ed). Wiley-VCH Verlag GmbH, Weinheim, Germany.
Jia F, Kacira M, Ogden KL. 2015. Multi-wavelength based optical density sensor for autonomous monitoring of microalgae. Sensors (Switzerland) 15 (9): 22234-22248. DOI: 10.3390/s150922234.
Kirrolia A, Bishnoi NR, Singh R. 2012. Effect of shaking, incubation temperature, salinity and media composition on growth traits of green microalgae *Chlorococcum* sp. J Algal Biomass Util 3 (3): 46-53.
Klausmeier CA, Litchman E, Daufresne T, Levin SA. 2004. Optimal nitrogen-to-phosphorus stoichiometry of phytoplankton. Nature 429 (6988): 171-174. DOI: 10.1038/nature02454.
Li Y, Chen M. 2015. Novel chlorophylls and new directions in photosynthesis research. Funct Plant Biol 42 (6): 493-501. DOI: 10.1071/FP14350.
Liang K, Zhang Q, Gu M, Cong W. 2013. Effect of phosphorus on lipid accumulation in freshwater microalga *Chlorella* sp. J Appl Phycol 25: 311-318. DOI: 10.1007/s10811-012-9865-6.
Liu N, Guo B, Cao Y, Wang H, Yang S, Huo H, Kong W, Zhang A, Niu S. 2021. Effects of organic carbon sources on the biomass and lipid production by the novel microalga *Micractinium reisseri* FM1 under batch and fed-batch cultivation. S Afr J Bot 139: 329-337. DOI: 10.1016/j.sajb.2021.02.028.
Liu W, Ming Y, Li P, Huang Z. 2012. Inhibitory effects of hypo-osmotic stress on extracellular carbonic anhydrase and photosynthetic efficiency of green alga *Dunaliella salina* possibly through reactive oxygen species formation. Plant Physiol Biochem 54: 43-48. DOI: 10.1016/j.plaphy.2012.01.018.
Luo L, He H, Yang C, Wen S, Zeng G, Wu M, Zhou Z, Lou W. 2016. Nutrient removal and lipid production by *Coelastrella* sp. in anaerobically and aerobically treated swine wastewater. Bioresour Technol 216: 135-141. DOI: 10.1016/j.biortech.2016.05.059.
Malla FA, Khan SA, Rashmi, Sharma GK, Gupta N, Abraham G. 2015. Phycoremediation potential of *Chlorella minutissima* on primary and tertiary treated wastewater for nutrient removal and biodiesel production. Ecol Eng 75: 343-349. DOI: 10.1016/j.ecoleng.2014.11.038.
Mulbry W, Kondrad S, Pizarro C, Kebede-Westhead E. 2008. Treatment of dairy manure effluent using freshwater algae: algal productivity and recovery of manure nutrients using pilot-scale algal turf scrubbers. Bioresour Technol 99 (17): 8137-8142. DOI: 10.1016/j.biortech.2008.03.073.
Pal D, Khozin-Goldberg I, Cohen Z, Boussiba S. 2011. The effect of light, salinity, and nitrogen availability on lipid production by *Nannochloropsis* sp. Appl Microbiol Biotechnol 90: 1429-1441. DOI: 10.1007/s00253-011-3170-1.
Pancha I, Chokshi K, Maurya R, Trivedi K, Patidar SK, Ghosh A, Mishra S. 2015. Salinity induced oxidative stress enhanced biofuel production potential of microalgae *Scenedesmus* sp. CCNM 1077. Bioresour Technol 189: 341-348. DOI: 10.1016/j.biortech.2015.04.017.
Pandit PR, Fulekar MH, Karuna MSL. 2017. Effect of salinity stress on growth, lipid productivity, fatty acid composition, and biodiesel properties in *Acutodesmus obliquus* and *Chlorella vulgaris*. Environ Sci Pollut Res 24 (15): 13437-13451. DOI: 10.1007/s11356-017-8875-y.
Pereira H, Gangadhar KN, Schulze PSC, Santos T, De Sousa CB, Schueler LM, Custódio L, Malcata FX, Gouveia L, Varela JCS, Barreira L. 2016. Isolation of a euryhaline microalgal strain, *Tetraselmis* sp. CTP4, as a robust feedstock for biodiesel production. Sci Rep 6: 1-11. DOI: 10.1038/srep35663.
Pozzobon V, Levasseur W, Guerin C, Gaveau-Vaillant N, Pointcheval M, Perré P. 2020. *Desmodesmus* sp. pigment and FAME profiles under different illuminations and nitrogen status. Bioresour Technol Rep 10: 100409. DOI: 10.1016/j.biteb.2020.100409.
Rawat I, Ranjith Kumar R, Mutanda T, Bux F. 2013. Biodiesel from microalgae: A critical evaluation from laboratory to large scale production. Appl Energy 103: 444-467. DOI: 10.1016/j.apenergy.2012.10.004.
Rees TAV, Cresswell RC, Syrett PJ. 1980. Sodium-dependent uptake of nitrate and urea by a marine diatom. Biochim Biophys Acta Biomembr 596 (1): 141-144. DOI: 10.1016/0005-2736(80)90178-9.
Ren HY, Liu BF, Kong F, Zhao L, Xie GJ, Ren NQ. 2014. Energy conversion analysis of microalgal lipid production under different culture modes. Bioresour Technol 166: 625-629. DOI: 10.1016/j.biortech.2014.05.106.
Ritchie RJ. 2006. Consistent sets of spectrophotometric chlorophyll equations for acetone, methanol and ethanol solvents. Photosynth Res 89 (1): 27-41. DOI: 10.1007/s11120-006-9065-9.
Sahle-Demessie E, Aly Hassan A, El Badawy A. 2019. Bio-desalination of brackish and seawater using halophytic algae. Desalination 465: 104-113. DOI: 10.1016/j.desal.2019.05.002.
Samorì G, Samorì C, Guerrini F, Pistocchi R. 2013. Growth and nitrogen removal capacity of *Desmodesmus communis* and of a natural microalgae consortium in a batch culture system in view of urban wastewater treatment: part I. Water Res 47 (2): 791-801. DOI: 10.1016/j.watres.2012.11.006.
Singh A, Ummalyma SB. 2020. Bioremediation and biomass production of microalgae cultivation in river water contaminated with pharmaceutical effluent. Bioresour Technol 307: 123233. DOI: 10.1016/j.biortech.2020.123233.
Singh R, Upadhyay AK, Chandra P, Singh DP. 2018. Sodium chloride incites reactive oxygen species in green algae *Chlorococcum humicola* and *Chlorella vulgaris*: implication on lipid synthesis, mineral nutrients and antioxidant system. Bioresour Technol 270: 489-497. DOI: 10.1016/j.biortech.2018.09.065.
Tamura K, Stecher G, Kumar S. 2021. MEGA11: Molecular Evolutionary Genetics Analysis Version 11. Mol Biol Evol 38 (7): 3022-3027. DOI: 10.1093/molbev/msab120.
Trivedi T, Jain D, Mulla NSS, Mamatha SS, Damare SR, Sreepada RA, Kumar S, Gupta V. 2019. Improvement in biomass, lipid production and biodiesel properties of a euryhaline *Chlorella vulgaris* NIOCCV on mixotrophic cultivation in wastewater from a fish processing plant. Renew Energy 139 (3): 326-335. DOI: 10.1016/j.renene.2019.02.065.
Ummalyma SB, Pandey A, Sukumaran RK, Sahoo D. 2018. Bioremediation by microalgae: current and emerging trends for effluents treatments for value addition of waste streams. In: Varjani S, Parameswaran B, Kumar S, Khare S (eds.) Biosynthetic Technol and Env Challenges. Springer, Singapore. DOI: 10.1007/978-981-10-7434-9_19.
von Alvensleben N, Magnusson M, Heimann K. 2016. Salinity tolerance of four freshwater microalgal species and the effects of salinity and nutrient limitation on biochemical profiles. J Appl Phycol 28 (2): 861-876. DOI: 10.1007/s10811-015-0666-6.
von Alvensleben N, Stookey K, Magnusson M, Heimann K. 2013. Salinity tolerance of *Picochlorum atomus* and the use of salinity for contamination control by the freshwater cyanobacterium *Pseudanabaena limnetica*. PLoS ONE 8 (5): e63569. DOI: 10.1371/journal.pone.0063569.
Yun CJ, Hwang KO, Han SS, Ri HG. 2019. The effect of salinity stress on the biofuel production potential of freshwater microalgae *Chlorella vulgaris* YH703. Biomass Bioenergy 127: 105277. DOI: 10.1016/j.biombioe.2019.105277.